Carbon nanotubes/graphene-like hybrid material for electrochemical determination of biomolecules

Fernando Francisco Muñoz[a,b]
[a]Departamento de Investigaciones en Sólidos
UNIDEF, CONICET, MINDEF , CITEDEF
[b]Consejo Nacional de Investigaciones Científicas y Técnicas (CONICET)
Buenos Aires, Argentina
fmunoz@citedef.gob.ar

María Celina Bonetto[b,c*]
[c]Instituto de Química y Fisicoquímica Biológica (IQUIFIB-CONICET)
Buenos Aires, Argentina
celinatt@yahoo.com.ar

***Abstract*— Glassy carbon electrodes (GC) were modified with multiwalled carbon nanotubes (CNT/GC) and were electrochemically treated to obtain a MWCNT/graphene-like hybrid material characterized via scanning electron microscopy (SEM), Raman spectroscopy, energy dispersive spectroscopy (EDS), and electrochemical techniques. These modified electrodes showed an electrochemical selective determination for dopamine (DA) and serotonin (5HT) in the presence of ascorbic acid (AA) and uric acid (UA).**

Keywords—carbon nanotubes; electrochemical treatment; hybrid material; biomolecules

I. Introduction

High electrical conductivity, large surface area, mechanical and chemical stability plus a reasonable cost of mass production are required for electrodes on behalf of electrochemical devices. Hence carbon nanotubes (CNTs) and graphene are some of the carbon allotropes most intensively explored in materials science for determination of biomolecules [1-3]. Graphene is a single atom thick, 2D sheet of sp^2 hybridized carbon atoms, densely packed in a honeycomb crystal lattice. Due to its structure, all of its atoms are on the surface, giving it an excellent biosensing potential in the nanoscale [4]. Its most important property is its excellent electrical conductivity, being a semiconductor with zero bandgap [5,6]. Any modification in the crystal lattice will alter its band structure. Particularly, a variation of the hybridization state of carbon atoms [7], other atoms or molecules incorporated in the lattice, and/or defects [8] can directly affect its electrical properties. The introduction of strong edge states and quantum confinement via structural constraints (nanoribbons, quantum dots, nanomesh) will have a similar effect [9]. CNTs are a sheet of graphene rolled into a well-ordered tube. Hence, an alternative way to obtain a graphene-like material is presented by Shinde et al. and their electrochemical approach to transform MWCNTs to reduced graphene nanoribbons (rGNRs) [10], simplifying experimental and waste disposal conditions [11]. Briefly, an electrochemical oxidation provides graphene oxide (GO) while the MWCNT get unzipped, supplying individual layers of GO that will turn into rGNRs upon reduction [10,12]. During oxidation, the sp^2 carbons are being continuously modified with O functionalities [13], to sp^3 carbons. The reduction of GO partially restores the sp^2 hybridization, improving the conductive behavior and yielding a graphene-like material [6]. Determination of DA and 5HT is important for early identification of diseases as depression, Parkinson, epilepsy, squizofrenia, or senile dementia, to minimize their deleterious effects [14,15]. The ability to monitor their physiological changes could also benefit the design of better and more efficient therapeutics. Due to DA and 5HT redox behavior, electrochemistry is suitable for their determination. However, some electroactive interferences such as AA and UA overlap their anodic peak potentials, between 0.2 and 0.35 V, with paste carbon electrodes [16-17]. In this work we report the fabrication and characterization of modified CNT/GC electrodes, electrochemically treated, to produce a 2D CNT/graphene-like hybrid material (rGNR/CNT/GC), and its application to simultaneous determination of DA and 5HT in the presence of AA and UA.

II. Materials and Methods

A. Reagents and instrumentation

All reagents were of analytical grade and used as received. MWCNTs were >98% carbon basis, 10 nm outer diameter, 4.5 nm inner diameter and 3.5 μm length. Phosphate buffered saline solution (PBS) was prepared in MilliQ water.

Electrochemical measurements were made with a standard three-electrode system, at room temperature (ca. 25 °C) in solutions deoxygenated with high purity N_2 using a Potentiostat/Galvanostat/ZRA (Series G 300TM and Interface 1000 from Gamry Instruments Inc. USA). A GC bare electrode (Structure Probe, Inc. PA, USA), or modified electrodes, were assayed as working electrodes. A Pt foil was used as counterelectrode. Two different reference electrodes (RE) were used, Ag/Ag_2SO_{4sat} or $Ag/AgCl_{sat}$. Solutions were used freshly prepared in MilliQ water.

Sonications were made using a Cole-Parmer ultrasonic bath.

SEM images were recorded on a SEM Carl Zeiss NTS SUPRA 40 (Carl Zeiss NTS GmbH, Germany). An Apollo X EDAX spectrophotometer (AMETEK, USA) was used.

Raman measurements were performed in a Confocal Horiba Jobin Yvon Dilor XY 800 (HORIBA Ltd, Japan).

B. Electrochemical treatment of MWCNT/GC

The GC electrodes (1 mm diameter) were pretreated via polishing with alumina powder on a wet cloth (0.3 μm), and then washed with water. Afterwards the electrodes were sonicated for 5 min in Milli-Q water and 5 min in ethanol and finally dried 15 min at 50 ºC. A dispersion of MWCNT (0.5 mg mL^{-1} of MWCNTs in absolute ethanol) was sonicated for 120 min. 5 μL of the dispersion were deposited onto a pretreated GC electrode, followed by drying at 50 ºC. CNT/GC were treated first by applying a fixed oxidation potential of +0.72 V for 6 h in 0.5 mol L^{-1} H_2SO_4 continuously deoxygenated with N_2 to obtain oCNT/GC. In

the second step oCNT/GC was treated by applying a fixed reduction potential of -0.75 V for 6 h in 0.5 mol L^{-1} H_2SO_4 continuously deoxygenated to obtain rGNR/CNT/GC.
An Ag/Ag_2SO_{4sat} was used as reference electrode for these electrochemical treatments of CNT/GC in H_2SO_4 to avoid Cl^- that may interfere in modified electrodes [19].

C. *Electrochemical characterization of the electrodes*

Electrochemical characterizations were made through cyclic voltammetry (CV) and electrochemical impedance spectroscopy (EIS) techniques using a $Ag/AgCl_{sat}$ RE. CV measurements were performed in PBS containing 5 mmol L^{-1} $Fe(CN)_6^{3-/4-}$, scanning the potential between -0.3 and 0.7 V with a scan rate of 50 mV s^{-1} or containing 1 mmol L^{-1} $Ru(NH_3)_6^{3+}$ scanning the potential between -0.5 and 0.2 V at 50 mV s^{-1}. EIS measurements were performed to a 5 mmol L^{-1} $Fe(CN)_6^{3-/4-}$ in PBS at 5 mV AC, 0.24 V DC, between 0.1 to 10^5 Hz, and 10 points/decade. Electrochemical surface areas (ECSA) were calculated by CV of 5 mmol L^{-1} $Fe(CN)_6^{3-}$ in 1 mol L^{-1} KCl, scanning the potential between -0.3 and 0.7 at 50 mV s^{-1}

D. *DPV measurements of 5HT, AA, DA, and UA*

Differential pulse voltammetry (DPV) was performed with modified and bare GC electrodes in samples with three different concentrations of 5HT, AA, DA and UA (in PBS) using an $Ag/AgCl_{sat}$ RE, and scanning the potential with a pulse size of 50 mV, step size of 5 mV, sample period of 0.35 s and pulse time of 0.05 s.

III. Results and Discussions

A. *SEM characterization*

The morphology of CNTs near GC surface (Figs. 1b and c) show some fused (circled in black) CNTs and some unzipped (circled in white) in treated electrodes (oCNT/GC and rGNR/CNT/GC), but not in CNT/GC (1a). It also show a significant width difference between oCNT/GC (Fig. 1b) and rGNR/CNT/GC (Fig. 1c) due to the O content in surface functionalities, the reduced ones being smaller; this width loss after reduction is used by some authors as criteria for effective reduction [20]. The fusion of CNTs may be due to a local increase of temperature as the oxidation potential is applied [21].

B. *Electrochemical oxidation of CNT/GC and reduction of oCNT/GC*

The electrochemical oxidation and reduction processes were followed through CV. It can be seen a quasireversible oxidation peak at 0.63 V that increased its height along with the oxidation of the CNTs (Fig. 2a) showing a versatile modified electrode with redox properties. Fig. 2b shows that an increase in the initial CV current (in absolute values) take place as long as the reduction potential is applied (-0.75V), evidencing a presumptive effective reduction.

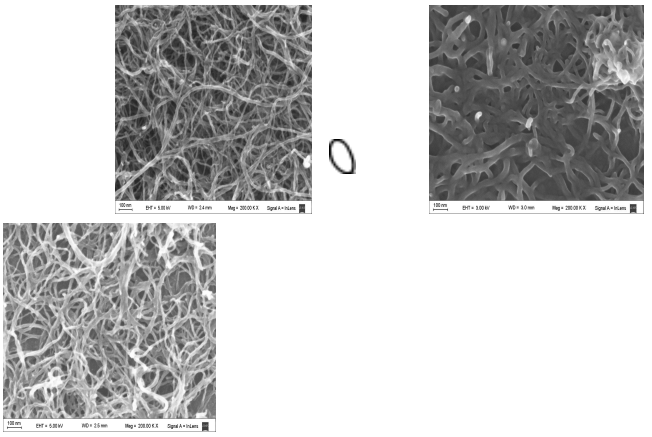

Fig. 1. SEM images of modified GC electrodes with CNT without any treatment (a), with oCNT (b), and with rGNR/CNT (c).

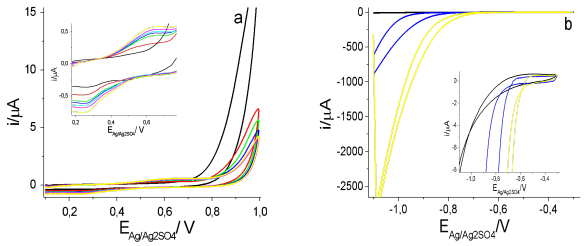

Fig. 2. (a) CV after oxidation of CNT/GC. (b) CV after reduction of oCNT/GC. 0 (black), 1 (red), 2 (green), 3 (blue), 4 (cyan), 5 (magenta) and 6 (yellow) hours. (100 mV s^{-1}). Zoom in insets.

C. *Raman spectroscopy analysis*

Raman spectroscopy revealed that the density of defects increased from CNT/GC to rGNR/CNT/GC after the electrochemical treatments, as shown in Fig. 2. The intensity of the defects (sp^3) related to peak D at 1350 cm^{-1} vs. the intensity of the peak G related to sp^2 hybridization (characteristic of graphitic-like materials) at 1560 cm^{-1} are a common tool among carbon based Raman spectra to determine the graphene character. The ratio I_D/I_G (Fig. 3) increased from 1 to 1.3 after the electrochemical oxidation of CNT, and the subsequent reduction process lowered that ratio down to 1.1 for the rGNR/CNT/GC electrode. The ratio increased upon oxidation of the CNT/GC owing to the unzipping of the CNTs, which generated a high number of defects (increasing peak D) coupled with O functionalization (note that peak G from rGNR/CNT/GC and oCNT/GC are practically alike).
It should be noted that the two processes are not necessarily coupled, nor the variations of the peaks are proportional [22], hence the decrease from 1.3 to 1.1 during reduction suggests the restitution of some sp^2 features. Additionally, the sharp peak 2D at 2700 cm^{-1} is only present in graphitic materials and is also a proof of graphene-like features [22]. In our case, peak 2D increases going from MWCNT to either their oxidized or reduced forms, in very good agreement with the intended transformation to a graphene-like material.

D. *EDS studies*

EDS analysis was used to confirm the C/O ratio in different modified electrodes. Its spectra showed that the O contained in oCNT/GC was (3.89 ± 0.18) at%, while rGNR/CNT/GC contained (2.05 ± 0.12) at% of O.

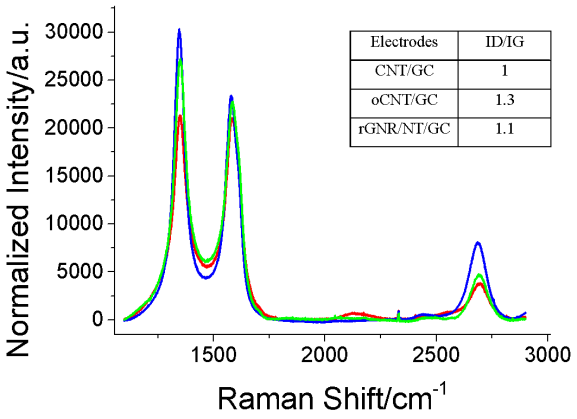

Fig. 3. Comparisons of Raman spectra of CNT/GC (red), oCNT/GC (blue) and rGNR/CNT/GC (green). Different ratios I_D/I_G are showed in the inset.

There were minimum differences between the at% of the O contained in the CNT/GC (1.72 ± 0.21) at% and the one contained in rGNR/CNT/GC, but there were big differences in the SEM images between both modified electrodes (Fig.1).

The ratio C/O is a complementary tool used to monitor the extent of graphitization [20] therefore the evaluation of this parameter shows an increase from 25:1, in oCNT/GC, to 48:1 in rGNR/CNT/GC, confirming a high degree of oxygen gropus reduction after treatment. These results, combined with the increase in the D band compared with CNT/GC (Raman) strongly suggest that the presence of a quasireversible oxidation peak in Fig. 1a corresponds to the CNTs oxidation after applying a potential of 0.72 V and the oCNTs reduction after the respective electrochemical treatment.

E. Electrochemical studies: $Fe(CN)_6^{3-/4-}$

$Fe(CN)_6^{3-/4-}$ were used to evaluate the electrodes performance since its reversibility assure that any due processes would be ascribable to the electrodes alone. Table 1 displays ΔEp values that are too high (much higher than the theoretical 1 electron transfer ΔEp expected of 59mV), very probably due to $Fe(CN)_6^{3-/4-}$ being an inner-sphere electrode reaction, known to have a surface-sensitive response, that can hinder its ability as a probe. Nevertheless, rGNR/CNT/GC show increased reversibility (the lowest ΔEp) and conductivity (the lowest R_{CT}) compared to the other modified electrodes (Table 1 and Fig. 4).

Values of electrochemical surface area (ECSA) were calculated based on Randles-Sevcik equation (1), assuming mass transport only by diffusion process (Table 1) [22].

$$Ip = 0.4463\, A\, c\, \gamma^{1/2} D^{1/2} RT^{-1/2} n^{3/2} F^{3/2} \quad (1)$$

The effective heterogeneous electron transfer (HET) rate constant, $k°_{eff}$, was determined via a method developed by Nicholson [23], applicable for quasi-reversible systems, calculated for each modified electrode, plotting against $[\pi\, Dn\, \nu\, F/(RT)]^{-1/2}$ as suggested by Brownson et al. [23]

TABLE 1. Values of ECSA and ΔEp using $Fe(CN)_6^{3-/4-}$. Calculated relative standard deviation, RSD, % in parenthesis (n=3).

Redox Couple	Electrode	ECSA / cm^2	ΔE_p / mV	R_{CT} / Ω
$Fe(CN)_6^{3-/4-}$	GC	0.0073±0.0006 (8.2)	100±9 (9)	1582±506 (31.9)
	CNT/GC	0.087±0.006 (6.9)	110±10 (9.3)	346±91 (26.3)
	oCNT/GC	0.071±0.005 (7)	110±6 (5.4)	132±9 (6.8)
	rGNR/CNT /GC	0.080±0.006 (7.5)	89±1 (1.1)	69±5 (7.2)

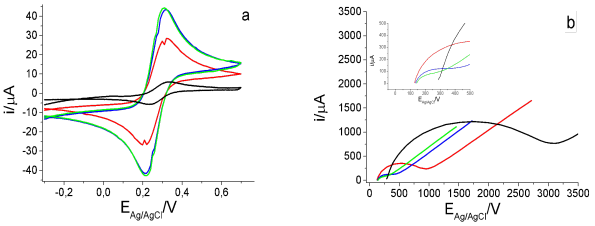

Fig. 4. (a) CV of $Fe(CN)_6^{3-/4-}$, (b) Nyquist plots of $Fe(CN)_6^{3-/4-}$, (inset: magnification of the high frequency zone). GC (black), CNT/GC (red), oCNT/GC (blue), and rGNR/CNT/GC electrodes (green).

where ψ is a kinetic parameter, D is the diffusion coefficient for $Ru(NH_3)_6^{3+}$, n is the number of electrons involved, F is the Faraday constant, R the gas constant, T the temperature, X being ΔEp and n the scan rate used (we used a range between 0.025 and 0.15 V). The kinetic parameter ψ was calculated with the following equation (2)

$$\psi = (-0.6288+0.0021\, X) / (1-0.017\, X) \quad (2)$$

The $k°_{eff}$ calculated for bare GC was $3.17\ 10^{-2}$, in good agreement with Brownson´s result [23]. Our rGNR/CNT/GC electrodes presented a $k°_{eff}$ of $3.2\ 10^{-1}$, a higher value than the calculated by Brownson with the EPPG electrode, therefore, coupled with stated results (Raman, EDS, ΔEp, R_{CT}) our modified electrodes based on graphene-like materials exhibit favorable electrochemical properties to be explored with biological molecules.

F. Electrochemical measurements of AA, DA, UA and 5HT

CNT/GC, or oCNT/GC electrodes presented poor selectivity in the presence of the four compounds AA, DA, UA, and 5HT (Fig. 5a) evidenced by the presence of only two peaks (only one peak was observed when GC electrodes were exposed to samples of the four analytes).

In contrast, four well-defined oxidation peaks, corresponding to AA, DA, UA and 5HT from left to right, were observed using the rGNR/CNT/GC (Fig. 5b).

The fact that the rGNR/CNT/GC electrode can resolve these four peaks is strong evidence of its improved selectivity towards these compounds. The restored sp^2 features of the rGNR/CNT/GC, combined with defects not restored with exposed oxygen groups and the presence of CNTs,

comprising a hybrid material electrode, clearly favors the selective oxidation of the four biological molecules tested.

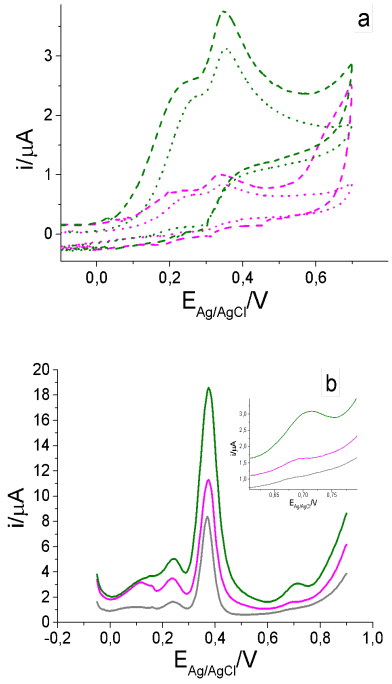

Fig. 5. DPV curves of three samples with AA, UA, DA and 5HT using a) CNT/GC (dot), oCNT/GC (dash) or b) rGNR/CNT/GC (solid). 4.6; 5; 50; 60 μmol L^{-1} (gray); 25, 25, 96; 120 μmol L^{-1} respectively (magenta); 90; 50; 245; and 240 μmol L^{-1} (olive) of 5HT, DA, UA and AA respectively (n=3). 5HT determination detail in the inset in b).

In DPV, the peak shape and height are criteria for kinetic capabilities of the reactions, with high and symmetric peaks corresponding to reversible or quasireversible kinetics [24,25].

The limit of detection (LOD) using rGNR/CNT/GC electrodes was calculated using the formula 3SD b^{-1} (SD is the standard deviation of 4 consecutive readings of the blank and b is the slope of the calibration plot of DA or 5HT). LOD for DA was calculated as 235 nmol L^{-1} and 460 nmol L^{-1} for 5HT. These detection limits are higher than other reported [14,17,26], but many of them do not inform the simultaneous determination of DA and 5HT in presence of AA and UA.

IV. Conclusions

In this work, an electrochemical treatment was applied to GC electrodes modified with a CNT/graphene-like hybrid material (rGNR/CNT/GC) in order to simultaneously determine DA and 5HT in presence of AA and UA. These modified electrodes, characterized through SEM, EDS, Raman spectroscopy, and electrochemical probes ($Fe(CN)_6^{3-/4-}$, $Ru(NH_3)_6^{2+/3+}$) may expose different morphologies to a sample, due to their surface modification with O functionalities and not recovered defects after the reduction step, guaranteeing mass transport and, as a consequence, performance enhancement, increasing conductivity and selectivity for DA and 5HT determination in presence of AA and UA [2]. Future work will focus on a deeper characterization of the modified electrodes, the electrodes processes, and the improvement of sensibility of DA and 5HT towards clinical determinations (eventually the determination of other biomolecules).

Acknowledgment

This work was supported by the University of Buenos Aires (IQUIBICEN-CONICET), the National Council for Scientific and Technological Research (CONICET, PIP 112-200801-00502), and the ANPCyT (Préstamo BID, PICT 2014-3407 and PICT 2014-0402).

References

[1] T.V. Magdesieva, P.V. Shvets, O.M. Nikitin, E.A. Obraztsova, F.T. Tuyakova, V.G. Sergeyev, A.R. Khokhlov, and A.N. Obraztsov, "Electrochemical characterization of mesoporous nanographite films", Carbon 105, 2016, pp. 96-102.

[2] S. Nardecchia, D. Carriazo, M.L. Ferrer, M.C. Gutiérrez, and F. del Monte, "Three dimensional macroporous architectures and aerogels built of carbon nanotubes and/or graphene: synthesis and applications", Chem. Soc. Rev. 42, 2013, pp. 794-830.

[3] C. Yang, M.E. Denno, P. Pyakurel, and B.J. Venton, "Recent trends in carbon nanomaterial based electrochemical sensors for biomolecules: A review", Anal. Chim. Acta. 887, 2015, pp. 17-37.

[4] M. Rahman, S. Beg, M.Z. Ahmad, F. Anwar, and V. Kumar, "Graphene and its diverse applications in healthcare systems", in: Graphene Science Handbook, Vol. 5, Sec. III, M. Aliofkhazraei, N. Ali, W.I. Milne, C.S. Ozkan, S. Mitura, J.L. Gervasoni (eds), CRC Press Taylor & Francis Group, 2016, p. 399.

[5] A. Pandikumar, G.T.S. How, T.P. See, F.S. Omar, S. Jayabal, K.Z. Kamali, N. Yusoff, A. Jamil, R. Ramaraj, S.A. John, H.N. Lim, and N.M. Huang, "Graphene and its nanocomposite material based electrochemical sensor platform for dopamine", RSC Adv. 4, 2014, pp. 63296-63323.

[6] T.S. Sreeprasad, and V. Berry, "How do the electrical properties of graphene change with its functionalization?", Small 9, 2013, pp. 341-350.

[7] D.C. Elias, R.R. Nair, T.M.G. Mohiuddin, S.V. Morozov, P. Blake, M.P. Halsall, A.C. Ferrari, D.W. Boukhvalov, M.I. Katsnelson, A.K. Geim, and K.S. Novoselov, "Control of graphene's properties by reversible hydrogenation: evidence for graphane", Science 323, 2009, pp. 610-613.

[8] D. Wei, Y. Liu, Y. Wang, H. Zhang, L. Huang, and G. Yu, "Synthesis of N-doped graphene by chemical vapor deposition and its electrical properties", Nano. Lett. 9, 2009, pp. 1752-1758.

[9] N. Mohanty, D. Moore, Z. Xu, T.S. Sreeprasad, A. Nagaraja, A.A. Rodriguez, and V. Berry, "Nanotomy-based production of transferable and dispersible graphene nanostructures of controlled shape and size", Nat. Commun. 3, 2012, pp. 1-8.

[10] D.B. Shinde, J. Debgupta, A. Kushwaha, M. Aslam, and V.K. Pillai, "Electrochemical unzipping of multi-walled carbon nanotubes for facile synthesis of high-quality graphene nanoribbons", J. Am. Chem. Soc. 133, 2011, pp. 4168-4171.

[11] D.V. Kosynkin, A.L. Higginbotham, A. Sinitskii, J.R. Lomeda, A. Dimiev, B.K. Price, and J.M. Tour, "Longitudinal unzipping of carbon nanotubes to form graphene nanoribbons", Nature 458, 2009, pp. 872-876.

[12] K.R. Sharma, "Synthesis methods for graphene" in: Graphene Science Handbook, Vol. 1, Sec. I, M. Aliofkhazraei, N. Ali, W.I. Milne, C.S. Ozkan, S. Mitura, J.L. Gervasoni (eds.), CRC Press Taylor & Francis Group, 2016, p. 31.

[13] X. Chang, F. Dong, Z. Tang, and F. Zha, "Construction of carboxyl functional groups and their enhancement effect for methanol electrocatalytic oxidation reaction", Int. J. Hydrog. Energy 44, 2019, pp. 27445-27454.

[14] H.S. Han, H.K. Lee, J-M. You, H. Jeong, and S. Jeon, "Electrochemical biosensor for simultaneous determination of dopamine and serotonin based on electrochemically reduced GO-porphyrin", Sens. Actuators B 190, 2014, 886-895.

[15] P. De Deurwaerdère, and G. Di Giovanni, "Serotonergic modulation of the activity of mesencephalic dopaminergic systems: Therapeutic implications", Prog. Neurobiol. 151, 2017, pp. 175-236.

[16] D.L. Robinson, A. Hermans, A.T. Seipel, and R.M. Wightman, "Monitoring rapid chemical communication in the brain", Chem. Rev. 108, 2008, pp. 2554-2584.

[17] T-Q. Xu, Q-L. Zhang, J-N. Zheng, Z-Y. Lv, J. Wei, A-J. Wang, and J-J. Feng, "Simultaneous determination of dopamine and uric acid in the presence of ascorbic acid using Pt nanoparticles supported on reduced graphene oxide", Electrochim. Acta 115, 2014, pp. 109-115.

[18] M. Velicky, K.Y. Tam, and R.A.W. Dryfe, "On the stability of the silver/silver sulfate reference electrode", Anal. Methods 4, 2012, pp. 1207-1211.

[19] S. Pei, and H.-M. Cheng, "The reduction of graphene oxide", Carbon 50, 2012, pp. 3210-3228.

[20] A.V. Krasheninnikov, and F. Banhart, "Engineering of nanostructured carbon materials with electron or ion beams", Nat. Mater. 6, 2007, pp. 723-733.

[21] D. Yoon, and H. Cheong, “Raman spectroscopy for characterization of graphene”, in: Raman Spectroscopy for Nanomaterials Characterization, Ch. 9, C.S.S.R. Kumar (ed.), Springer, 2012, p. 191.
[22] L. Wang, and Y. Yamauchi, “Facile synthesis of three-dimensional dendritic platinum nanoelectrocatalyst”, Chem. Mater. 21, 2009, 3562-3569.
[23] D.A.C. Brownson, P.J. Kelly, and C.E. Banks, “In situ electrochemical characterisation of graphene and various carbon-based electrode materials: an internal standard approach”, RSC Adv. 5, 2015, 37281-37286.
[24] A.J. Bard, and L.R. Faulkner, “Electrochemical Methods, Fundamentals and Applications”, Ch. 3, John Wiley & Sons, 2001.
[25] C.M.A. Brett, and A.M. Oliveira Brett, “Electrochemistry Principles, Methods, and Applications”, Part I, Oxford University Press, 1993.
[26] S. Qi, B. Zhao, H. Tang, and X. Jiang, “Determination of ascorbic acid, dopamine, and uric acid by a novel electrochemical sensor based on pristine graphene”, Electrochim. Acta 161, 2015, 395-402.